Coupling of ferromagnetism and structural phase transition in V2O3/Co bilayers

Wang, C.; Xu, C.; Wang, M.; Yuan, Y.; Liu, H.; Dillemans, L.; Homm, P.; Menghini, M.; Locquet, J.-P.; Haesendonck, C. V.; Zhou, S.; Ruan, S.; Zeng, Y.-J.;

Originally published:

November 2017

Journal of Physics D: Applied Physics 50(2017), 495002

DOI: https://doi.org/10.1088/1361-6463/aa9607

Manuscript submitted to Journal of Physics D: Applied Physics

Coupling of ferromagnetism and structural phase transition in V_2O_3/Co bilayers

Changan Wang,[1,2] Chi Xu,[2] Mao Wang,[2] Ye Yuan,[2] Haoliang Liu,[3a)] Leander Dillemans,[3] Pía Homm,[3] Mariela Menghini,[3] Jean-Pierre Locquet,[3] Chris Van Haesendonck,[3] Shengqiang Zhou,[2] Shuangchen Ruan,[1] and Yu-Jia Zeng [1b)]

1）Shenzhen Key Laboratory of Laser Engineering, College of Optoelectronic Engineering, Shenzhen University, 518060 Shenzhen, China

2）Helmholtz-Zentrum Dresden-Rossendorf, Institute of Ion Beam Physics and Materials Research, Bautzner Landstr. 400, 01328 Dresden, Germany

3) Laboratory of Solid-State Physics and Magnetism, KU Leuven, Celestijnenlaan 200 D, BE-3001 Leuven, Belgium

a) *E-mail:* liuhaoliang03@gmail.com(H.-L. Liu)

b) *E-mail:* yjzeng@szu.edu.cn (Y.-J. Zeng)

ABSTRACT

Interfacial coupling in hybrid magnetic heterostructures is being considered as a unique opportunity for functional material design. Here, we present the temperature dependence of magnetic properties of V_2O_3/Co bilayers influenced by the structural phase transition that is accompanied by a metal-insulator transition in V_2O_3. Both the coercivity and the magnetization of Co layer are strongly affected by the interfacial stress due to the magnetostrictive effect in the ferromagnetic film. The observed change in coercivity is as large as 59% in a narrow temperature range. The changes in the magnetic properties are reproducible and reversible, which are of importance for potential applications.

Keywords: Magnetostrictive coupling, Metal-insulator transition, Structural phase transition, Heterostructure

I. Introduction

Manipulating magnetic properties of ferromagnetic (FM) layers through stimuli other than a magnetic field has attracted a lot of research attention in recent years due to its potential for device applications [1-3]. Examples of external stimuli include electric field, electric current, pressure and light, which open new routes to tune the properties of magnetic materials in a controlled way [3-8]. Thin-film hybrid structures are particularly sensitive to external stimuli and they are ideal platforms to investigate the underlying physical mechanisms dominating the properties of magnetoelectric heterostructures, such as ferromagnetic/multiferroic, piezoelectric/ferromagnetic and ferroelectric/ferromagnetic heterostructures [9-11]. One promising approach that can exploit the manipulation of the magnetic properties is provided by placing a ferromagnet in proximity to materials that undergo a structural phase transition (SPT) accompanied by a metal-insulator transition (MIT) [5, 12-15]. In this case, the MIT and SPT can be induced not only by changing temperature, but also can be driven by pressure, light or electric current [5]. Therefore, these materials offer the possibility to tune the magnetic properties of the ferromagnetic layer by multiple stimuli.

Among all the materials that show a MIT and SPT, vanadium sesquioxide (V_2O_3) is one of the most fascinating systems due to its rich phase diagram [16, 17]. V_2O_3 shows a first-order phase transition (at ~160 K) from a high temperature metallic state to a low-temperature insulating state [18]. The change in resistance can be as large as 7 orders of magnitude across the MIT [5]. These remarkable features are associated with a SPT from a rhombohedral crystal structure in the metallic phase to a monoclinic crystal structure in the insulating phase that occurs simultaneously with the electronic phase transition [13]. The crystallographic change occurring in V_2O_3 provides the possibility to achieve reversible manipulation of the magnetic properties of the FM layer in hybrid thin-film through the magnetoelastic anisotropy that is induced by phase coexistence at the nanoscale in the MIT

material and the interfacial stress within the transition temperature range. As already reported in literature [12, 13, 15], the proximity of FM layers, such as Fe, Co or Ni, to V_2O_3 and VO_2 affects the magnetic and electronic properties at the interface between FM and SPT materials. Hence, combining V_2O_3 film with a ferromagnetic Co film in a bilayer configuration provides a unique way to investigate the coupling effect when the oxide undergoes a SPT accompanied by a MIT. However, the coupling effect between V_2O_3 and Co has not been studied in detail.

In this paper, we describe the fabrication of V_2O_3/Co bilayers grown by molecular beam epitaxy (MBE) and investigate their temperature-dependent magnetic properties. We find that the ferromagnetic properties of the Co thin film in the bilayers are strongly affected by interfacial stress associated with the SPT accompanied by a MIT in V_2O_3. Reversible changes are observed for the coercivity and magnetization across the SPT in the V_2O_3 film. This effect results in a reproducible modification of magnetic properties, which is of direct relevance for technological applications.

II. Experimental details

The V_2O_3/Co bilayers are grown by MBE in a chamber with a base pressure of 1×10^{-9} mbar. 30-nm-thick V_2O_3 films are deposited on (0001)-Al_2O_3 substrates at a temperature of 742 °C and in an oxygen partial pressure of 8.3×10^{-7} mbar. 5-nm-thick Co films are then ex-situ deposited on the V_2O_3 thin films as well as on bare Al_2O_3 substrates at room temperature and at a base pressure of 5×10^{-9} mbar [19]. To prevent oxidization, 3 nm of Au is deposited in-situ as capping layer on top of the Co layer. The thin-film samples are characterized by means of high resolution X-ray diffraction (XRD) using Cu Kα radiation. The surface morphology of the Co film on V_2O_3 is characterized by *in-situ* scanning tunneling microscopy (STM) before capping with Au. The temperature-dependence of the resistance of the V_2O_3 film is measured using a four-probe geometry and a constant current source. Temperature is swept at a slow rate of 1-2 K/min with a Lakeshore 332 temperature controller. Magnetic properties are

measured with a superconducting quantum interference device magnetic property measurement system (SQUID-MPMS, Quantum Design).

III Results and discussion

In Fig. 1(a) we present the XRD scan for a 30 nm-thick V_2O_3 film grown on an (0001) oriented Al_2O_3 substrate. It is obvious that the sample shows good crystalline quality and the absence of any secondary phase. In this case, only the peak corresponding to the (0006) plane of V_2O_3 is observed, indicating that the V_2O_3 film grows epitaxially on the substrate along the (0001) orientation. To determine the microscopic structure of the Co film, we present in Fig.1(b) the STM image of a 5-nm-thick Co layer on V_2O_3. Nearly circular, coalescing Co grains are observed with typical size smaller than 8 nm and with a RMS roughness of 0.52nm. The inset of Fig. 1(b) shows the height profile across the line indicated in the 2D map. The RSM roughness and height profile confirm the successful preparation of the V_2O_3/Co bilayers, which allows performing a reliable investigation of the heterostructural magnetic properties.

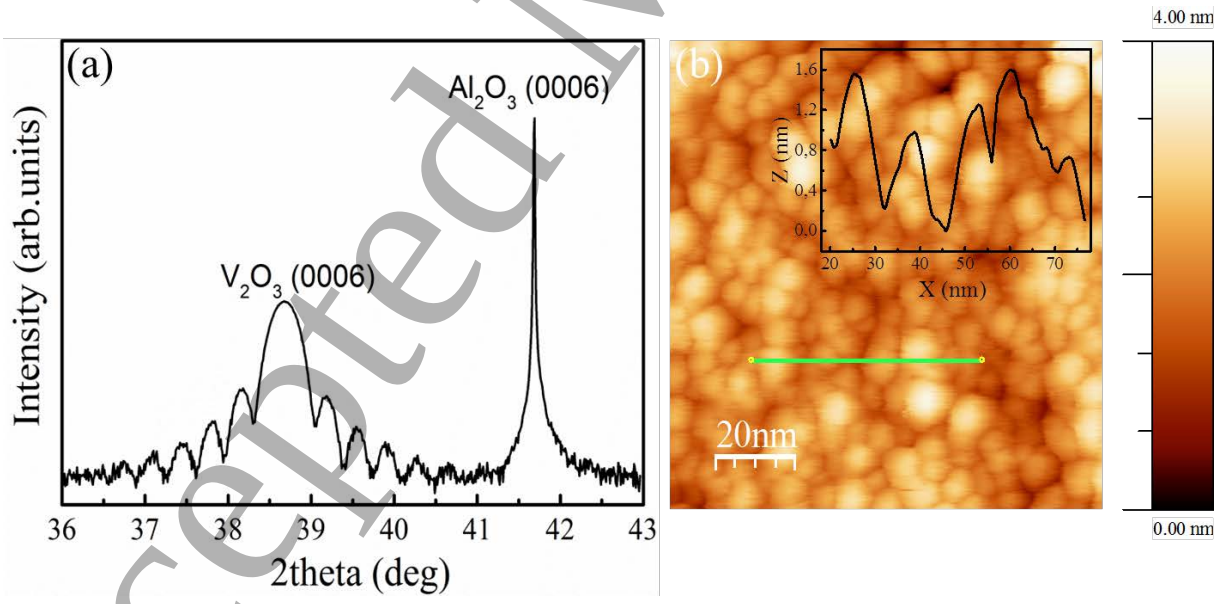

Fig. 1. (a) XRD $\theta/2\theta$ scans for a 30 nm-thick V_2O_3 film grown on an Al_2O_3 substrate. (b) Surface morphology of a 5-nm-thick Co film on top of a 30-nm-thick V_2O_3 film as measured by STM. Inset shows the height profile along the line in (b) and the extracted RSM roughness is 0.52 nm.

To investigate the coupling between V_2O_3 and Co, the magnetization curves of the V_2O_3

/Co bilayers are measured at different temperatures near the SPT in the V_2O_3. The results are plotted in Fig. 2(a). All curves show a ferromagnetic behavior with varying coercivity, originating from the top Co layer. Fig. 2(b) summarizes the dependence of the coercive field H_c on temperature for the V_2O_3 /Co bilayer compared to a reference Co film grown directly on Al_2O_3. For the Co reference film, we observe the standard (almost) linear dependence of the coercivity on temperature. For the bilayers, however, a strong deviation from the linear behavior of H_c occurs within a narrow temperature range (160 K - 185 K). For temperatures higher than 185 K, H_c of the bilayer is almost the same as of the Co layer. However, an increase in H_c of ~59% (from 92 Oe at 185 K to 146 Oe at 160 K) is observed in the bilayer while the change in the same temperature range for the Co film is of only ~15%. Interestingly, the deviation in H_c is observed within a temperature range where the V_2O_3 structural phase transition occurs (in this temperature range the V_2O_3 layer exhibits a MIT, see Fig. 3(a)) [13, 20]. On the other hand, the coercive field in the V_2O_3 /Co bilayers is slightly larger for increasing than for decreasing temperature (see inset in Fig. 2(b)), which can be attributed to the typical thermal hysteresis observed for the structural phase transition in V_2O_3 [12]. However, when the temperature is below 160 K and above 185 K, i.e. outside of the phase transition region, the coercivity shows a quasi-linear dependence on temperature and it is independent of the temperature sweep direction. We therefore can conclude that the observed anomalous ferromagnetism in the thin Co films is associated with the SPT in the adjacent V_2O_3 thin film.

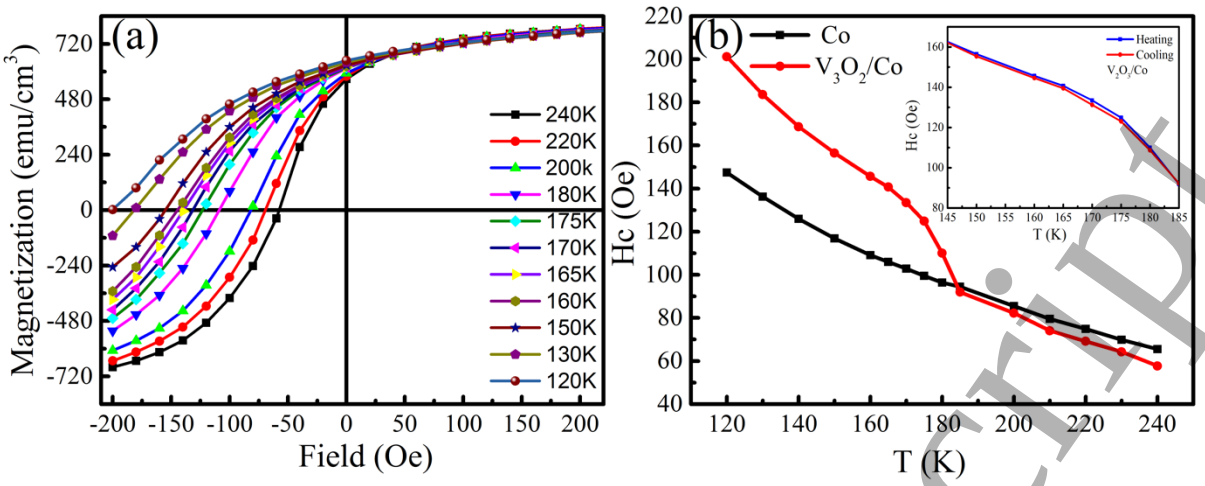

Fig. 2. (a) In-plane M-H curves of a V_2O_3/Co bilayer at different temperatures near the structural phase transition in the V_2O_3 film. (b) Coercivity versus temperature for a V_2O_3/Co bilayer compared to a reference Co film. The inset in (b) shows the coercivity dependence on temperature between 145 K and 185 K.

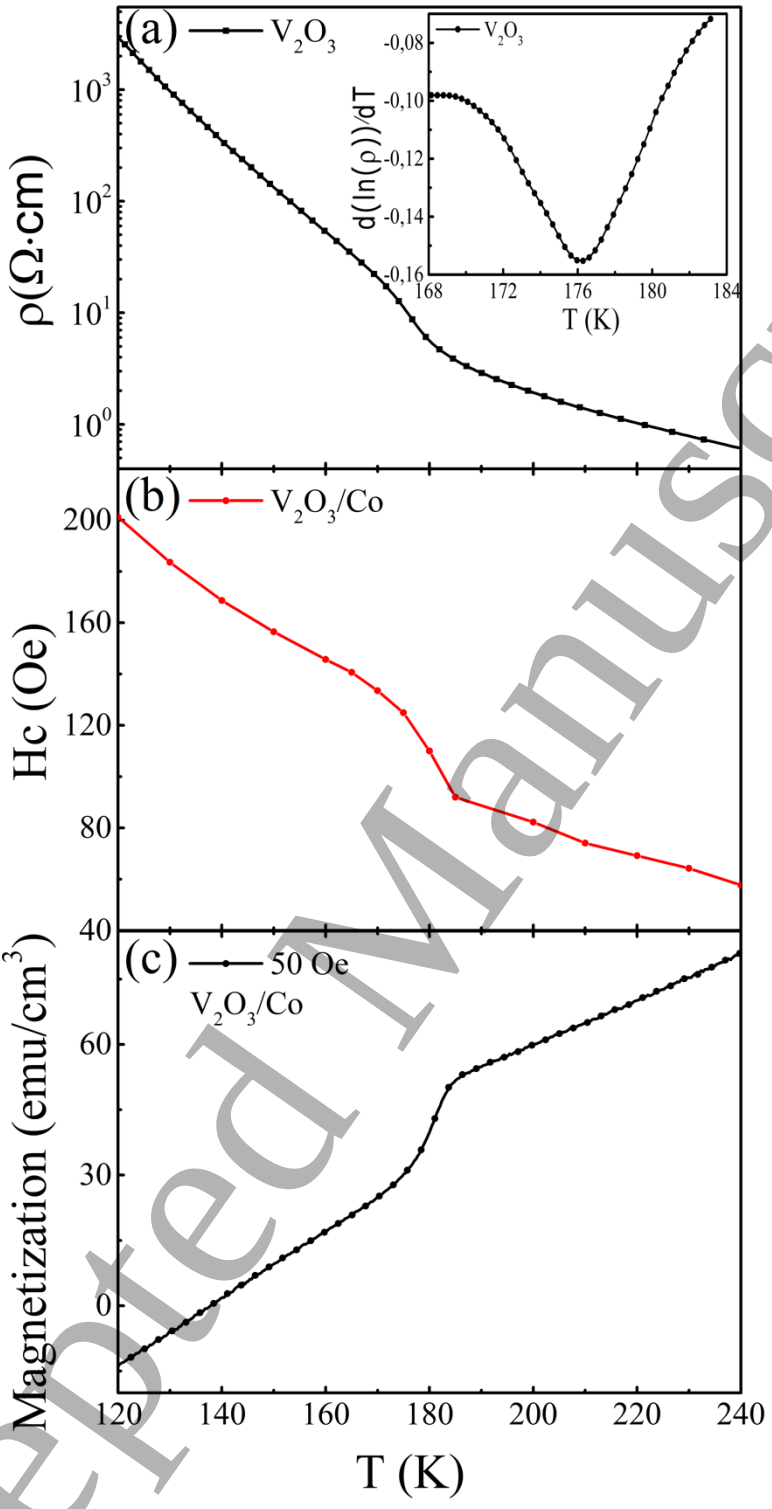

Fig. 3. (a) Resistivity as a function of temperature for the V_2O_3 film. Inset shows the differential curves of resistivity vs temperature to indicate the transition temperature of 176 K. (b) Coercivity versus temperature and (c) ZFC magnetization measured at 50 Oe as a function of temperature for a V_2O_3/Co bilayer.

In Fig. 3(a) we present the resistivity as a function of temperature for a V_2O_3 film. One can

see that a typical MIT is observed for our V_2O_3 films, which is similar to previous reports for V_2O_3 [20, 21]. The transition temperature (T_{MIT}) is determined from the derivative of *ln*(ρ) and plotted with respect to temperature, as shown in the inset of Fig. 3(a). The plot shows a clear peak, indicating T_{MIT} in resistivity at 176 K. Fig. 3(b) summarizes the dependence of the coercive field on temperature for the V_2O_3 /Co bilayer. It indicates the deviation from the linear behavior in the temperature range where the V_2O_3 SPT occurs. In Fig. 3(c) we present the behavior of the zero-field-cooled (ZFC) magnetization as a function of temperature in the presence of a 50 Oe magnetic field. It is evident that an anomaly in the magnetization occurs within the same temperature range where the deviation from the linear behavior of the coercivity is observed. Hence, the MIT and SPT are centered approximately at the same temperature at which the behavior of the coercivity and magnetization with temperature deviate from the Co reference film. Thus, the magnetic properties of the Co layer can be modified by relying on the SPT and MIT in the adjacent V_2O_3 layer. Note that the transition in resistivity typically spans a broad region in Fig. 3(a). This is because the transition in resistivity with decreasing temperature goes through four successive stages: a homogenous metallic state, a striped nanotexture of percolating electronic phase coexistence, an inhomogeneous correlated insulator state and a homogeneous insulator state [18]. As described in Ref. [18], in the region of coexistence of insulating and metallic domains below the bulk T_{MIT}, the transport is influenced by percolation.

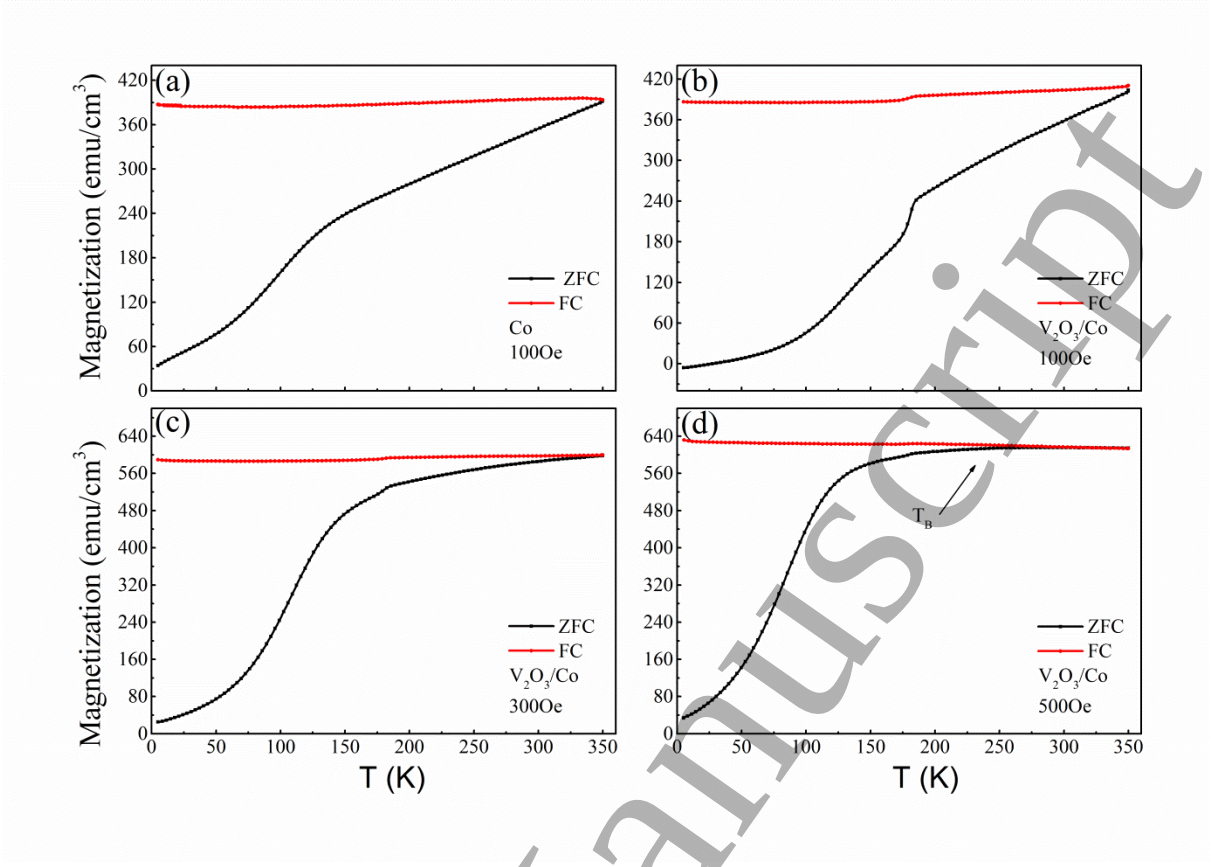

Fig. 4. The ZFC and FC magnetization measured for (a) a Co film at 100 Oe and (b) a V_2O_3/Co bilayer at 100 Oe, (c) 300 Oe and (d) 500 Oe. Note that the blocking temperature T_B is indicated only for a field of 500 Oe. For other fields T_B is above 350 K.

In Fig. 4 the zero-field-cooled (ZFC) and field-cooled (FC) magnetization curves of a Co thin film at 100 Oe and of the V_2O_3/Co bilayer at different magnetic fields are shown. Since the contribution of the V_2O_3 to magnetization is negligible, all curves have been normalized with respect to the Co volume. From Fig. 4(a) it is clear that the Co thin film shows splitting of the ZFC and FC, which is likely due to the small size of Co grains contained in the film. The magnetization reveals a superparamagnetic behavior with "blocking" occurring at a temperature higher than 350 K [22]. On the other hand, it is noticeable that there is a different behavior in the magnetization of the bilayers as already shown in Fig. 3(c) (see Fig. 4(b)). The magnetization (both in the ZFC and FC curves) shows a small kink in the same temperature range where the deviations from the linear behavior in the coercivity are observed, as shown in Fig. 3(b). This further indicates that both effects are closely related to the SPT in the V_2O_3

thin film. In Fig. 4 (b) and (c) the splitting between the ZFC and FC magnetization at different magnetic fields disappears at higher temperatures, which can be attributed to a superparamagnetic behavior resulting from the presence of small Co grains (see Fig. 1(b)). We note that the ZFC magnetization gradually increases (grains become unblocked) until reaching the average blocking temperature T_B, while the FC curves slowly decrease with increasing temperature. Moreover, it is evident that T_B tends to shift to lower temperatures when the applied magnetic field increases. This is expected and can be accounted for the fact that a larger magnetic field tends to reduce the energy barriers that hinder the fluctuation of magnetic moment, resulting in a transition to a thermally unfrozen state at lower temperatures.

As indicated above, another interesting finding is that the kink in magnetization, which is observed within the temperature interval where the SPT in the V_2O_3 thin film occurs, gradually vanishes when increasing the applied magnetic field, as illustrated in Fig. 4 and Fig. 3(c). Moreover, when the applied magnetic field is relatively low, these striking changes in the magnetization as function of temperature indicate that the Co magnetization may be not fully saturated. On the other hand, the SPT in V_2O_3 appears to play a crucial role to induce these changes in the magnetic behavior of the V_2O_3 /Co bilayers. It is well known that the magnetism of magnetic metal atoms is susceptible to an environment with fewer nearest neighbor atoms [23]. For example, surface atoms can reveal a strong magnetic polarization, while the bulk atoms have a smaller magnetic moment. Hence, the weaker interatomic hybridization at the V_2O_3/Co interface is likely to influence the magnetization of Co atoms at the interface. The symmetry and coordination number at the interface of the bilayers can be changed due to the SPT in the V_2O_3 film, which induces a narrowed *d*-band and therefore localizes surface states or surface resonance states in the Co atoms. This then results in a significantly stronger magnetic polarization in the interface region and can induce an anomaly in the magnetization for small applied magnetic fields [23, 24]. When the applied magnetic field is, however, increased to 500 Oe, the results in Fig. 4 (d) illustrate that the coupling

effect at the interface is suppressed and the magnetization of the Co layer is not affected by the SPT in the V_2O_3 layer. This indicates that the effect of weakened interatomic hybridization near the V_2O_3 /Co interface becomes suppressed by the external magnetic field at which the Co may also be fully saturated.

As we mentioned above, the remarkably reproducible modification of the coercivity is also a result of the SPT in the V_2O_3 layer, which is accompanied by a MIT. The V_2O_3 SPT gives rise to a 1.4 % volume increase when undergoing a transition from a rhombohedral phase at higher temperature to a monoclinic phase at lower temperature [21]. The volume expansion leads to epitaxial stress in the adjacent FM Co layer, thus changing the magnetic properties by an inverse magnetostrictive effect. The magnitude of the stress that produces the variations in coercivity shown in Fig. 2(b) can be estimated from the stress anisotropy field $H_{K\sigma,}$ which is given by: [25]

$$H_{K\sigma} = \frac{3\lambda_{si}\sigma}{M_S} \quad (1)$$

where λ_{si} is the saturation magnetostriction, σ is the stress in MPa, and M_S is the saturation magnetization in G or emu/cm^3. The observed value of coercivity at 120 K, at which the SPT is expected to be completed, is 147 Oe and 201 Oe in the single Co film and the bilayer, respectively [see Fig. 2(b)]. The additional anisotropy coercivity produced by the coupling effect is then 54 Oe. We calculate M_S to be 632 emu/cm^3 according to the results presented in Fig. 2(a). However, there are large variations of reported λ_{si} values for Co, ranging from ~ -11×10^{-6} to -95×10^{-6} [25-28]. Also, the Co layer is likely to be a collection of coalesced nanoparticles forming a continuous film. We therefore cannot make a good estimate of the stress produced by the V_2O_3 layer according to the Equation (1), nor can we make a comparison with the coupling of a VO_2/Ni layer, which produces a σ= 589 MPa across the SPT [12]. However, we expect a stronger coupling effect when the Co films are grown in-situ on top of the V_2O_3 films.

IV. Conclusion

We observe magnetostrictive coupling across the interfaces of hybrid magnetic heterostructures. The coupling is caused by the interfacial stress induced by the structural phase transition accompanied by the metal-insulator transition in the V_2O_3 film, which causes pronounced changes in the magnetic properties of V_2O_3/Co bilayers due to the magnetostrictive effect. The change in coercivity is as large as 59% within a narrow temperature range across the transition. The reversible modification of the magnetic properties of ferromagnets opens up new possibilities for technological applications in which relevant ferromagnetic properties, such as magnetization and coercivity, can be tailored for desired applications.

Acknowledgments

This work was supported by the National Natural Science Foundation of China under Grant No. 51502178, the Shenzhen Science and Technology Project under Grant No. JCYJ20150324141711644 and the Natural Science Foundation of SZU. C. A. Wang, C. Xu, M. Wang and Y. Yuan thank China Scholarship Council for financial supports. P. Homm acknowledges support from Becas Chile-CONICYT. We are thankful to Dr. Jörg Grenzer for discussions.

References

[1] Cherifi R, Ivanovskaya V, Phillips L, Zobelli A, Infante I, Jacquet E, Garcia V, Fusil S, Briddon P, and Guiblin N 2014 *Nat. Mater.* **13** 345-51.

[2] Chernyshov A, Overby M, Liu X, Furdyna J K, Lyanda-Geller Y, and Rokhinson L P 2009 *Nat. Phys.* **5** 656-9.

[3] Kirilyuk A, Kimel A V, and Rasing T 2010 *Rev. Mod. Phys.* **82** 2731.

[4] Vaz C A 2012 *J. Phys.: Condens. Matter.* **24** 333201.

[5] Yang Z, Ko C, and Ramanathan S 2011 *Annu. Rev. Mater. Res.* **41** 337-67.

[6] Kim J, Sinha J, Hayashi M, Yamanouchi M, Fukami S, Suzuki T, Mitani S, and Ohno H 2013 *Nat. Mater.* **12** 240-5.

[7] Rokhinson L P, Overby M, Chernyshov A, Lyanda-Geller Y, Liu X, and Furdyna J K 2012 *J. Magn. Magn. Mater.* **324** 3379-84.

[8] Saranu S, Selve S, Kaiser U, Han L, Wiedwald U, Ziemann P, and Herr U 2011 *Beilstein. J. Nanotech.* **2** 268-75.

[9] Heron J, Trassin M, Ashraf K, Gajek M, He Q, Yang S, Nikonov D, Chu Y, Salahuddin S, and Ramesh R 2011 *Phys. Rev. Lett.* **107** 217202.

[10] Geprägs S, Brandlmaier A, Opel M, Gross R, and Goennenwein S 2010 *Appl. Phys. Lett.* **96** 142509.

[11] Mardana A, Ducharme S, and Adenwalla S 2011 *Nano. Lett.***11** 3862-7.

[12] De La Venta J, Wang S, Ramirez J, and Schuller I K 2013 *Appl. Phys. Lett.* **102** 122404.

[13] De La Venta J, Wang S, Saerbeck T, Ramírez J, Valmianski I, and Schuller I K 2014 *Appl. Phys. Lett.* **104** 062410.

[14] Saerbeck T, de la Venta J, Wang S, Ramírez J G, Erekhinsky M, Valmianski I, and Schuller I K 2014 *J. Mater. Res.* **29** 2353-65.

[15] Sass B, Tusche C, Felsch W, Bertran F, Fortuna F, Ohresser P, and Krill G 2005 *Phys. Rev. B.* **71** 014415.

[16] Sakai J, Limelette P, and Funakubo H 2015 *Appl. Phys. Lett.* **107** 241901.

[17] Hansmann P, Toschi A, Sangiovanni G, Saha‐Dasgupta T, Lupi S, Marsi M, and Held K 2013 *Phys. Status. Solidi. B.* **250** 1251-64.

[18] McLeod A, van Heumen E, Ramirez J, Wang S, Saerbeck T, Guenon S, Goldflam M, Anderegg L, Kelly P, and Mueller A 2017 *Nat. Phys.***13** 80-86.

[19] Liu H-L, Brems S, Zeng Y-J, Temst K, Vantomme A, and Van Haesendonck C 2016 *J. Phys.: Condens. Matter* **28** 196002.

[20] Dillemans L, Smets T, Lieten R, Menghini M, Su C-Y, and Locquet J-P 2014 *Appl. Phys. Lett.* **104** 071902.

[21] McWhan Dand Remeika J 1970 *Phys. Rev. B.* **2** 3734.

[22] Li D, Zeng Y, Pereira L, Batuk D, Hadermann J, Zhang Y, Ye Z, Temst K, Vantomme A, and Van Bael M 2013 *J. Appl. Phys.* **114** 033909.

[23] Freeman Aand Wu R-q 1991 *J. Magn. Magn. Mater.***100** 497-514.

[24] Hattox T M, Conklin J, Slater J, and Trickey S 1973 *J. Phys. Chem. Solids* **34** 1627-38.

[25] Cullity B Dand Graham C D. Introduction to Magnetic Materials: *John Wiley & Sons* 2009.

[26] Klokholm E, and Aboaf J 1982 *J. Appl. Phys.* **53** 2661.

[27] Lee E W 1955 *Rep. Prog. Phys.* **18** 184.

[28] Bozorth R M 1954 *Phys. Rev.* **96** 311.